Communications Research Centre

PRELIMINARY COVERAGE STUDIES FOR SPACE-BASED RADAR SURVEILLANCE AND TRACKING

by
B.J. Rook

AUGUST 1983

This work was sponsored by the Department of National Defence, Research and Development Branch under Project No. 33C81.

CRC REPORT NO. 1363

Government of Canada
Department of Communications

Gouvernement du Canada
Ministère des Communications

Canada

COMMUNICATIONS RESEARCH CENTRE

DEPARTMENT OF COMMUNICATIONS
CANADA

PRELIMINARY COVERAGE STUDIES FOR SPACE-BASED RADAR SURVEILLANCE AND TRACKING

by

B.J. Rook

(Radar and Communications Technology Branch)

CRC REPORT NO. 1363

August 1983

OTTAWA

This work was sponsored by the Department of National Defence, Research and Development Branch under Project No. 33C81.

TABLE OF CONTENTS

PRELIMINARY COVERAGE STUDIES FOR SPACE-BASED RADAR SURVEILLANCE AND TRACKING

by

B.J. Rook

ABSTRACT

A time-based computer simulation of space-based radar (SBR) systems is described. This simulation models the orbital dynamics of multiple radar satellites and computes the instantaneous fields of view of hypothetical on-board surveillance radars. The procedures are illustrated by computer-generated graphical examples. Preliminary coverage studies have been carried out for various satellite configurations, and illustrative results from these studies are provided to demonstrate the usefulness of this simulation in evaluating the performance of SBR systems.

INTRODUCTION

The purpose of this report is to present some illustrative results from a preliminary study of the performance of Space-Based Radar (SBR) systems intended for the surveillance and tracking of air-breathing targets. This study is concerned with radar coverage areas on the surface of the Earth and with the constellation of satellites required to provide continuous coverage for different orbital configurations.

In Part A, the mathematics necessary to describe the orbital dynamics of space vehicles is reviewed, and a computational procedure is developed using matrix transformations of co-ordinate components to simulate orbiting satellites about a rotating Earth. Examples are then presented to illustrate this procedure.

In Part B, fields of view for hypothetical SBR systems are computed using this procedure from which coverage diagrams are presented and examined. The computer-based analytical tool is then used to obtain coverage statistics for various satellite configurations.

The time-based simulation of the satellite-Earth dynamics will form part of more detailed SBR simulations, in which the space-based radar characteristics (power, aperture), the target characteristics (radar cross-section, flight scenario) and the detection and interference conditions (Earth clutter, jamming) will be taken into account. The corresponding results will be presented in a future report.

PART A - SATELLITE-EARTH DYNAMICS

A1 DYNAMICS OF ORBITING SATELLITES

A1.1 Elliptical Orbits

The motion of an orbiting satellite is assumed to obey the unperturbed laws of Kepler. This means that the Earth is represented by a homogeneous sphere with all its mass concentrated at the centre. The orbit of the satellite is then a perfect ellipse as depicted in Figure 1, where:

0 = the centre of the Earth where its mass is concentrated;

R_1 = the distance from the centre of the Earth to the perigee, the perigee being the point at which the satellite is closest to the mass;

R_2 = the distance from the centre of the Earth to the apogee, the apogee being the point at which the satellite is furthest from the mass;

a = length of the semi-major axis of the ellipse;

C = the semi-focal length.

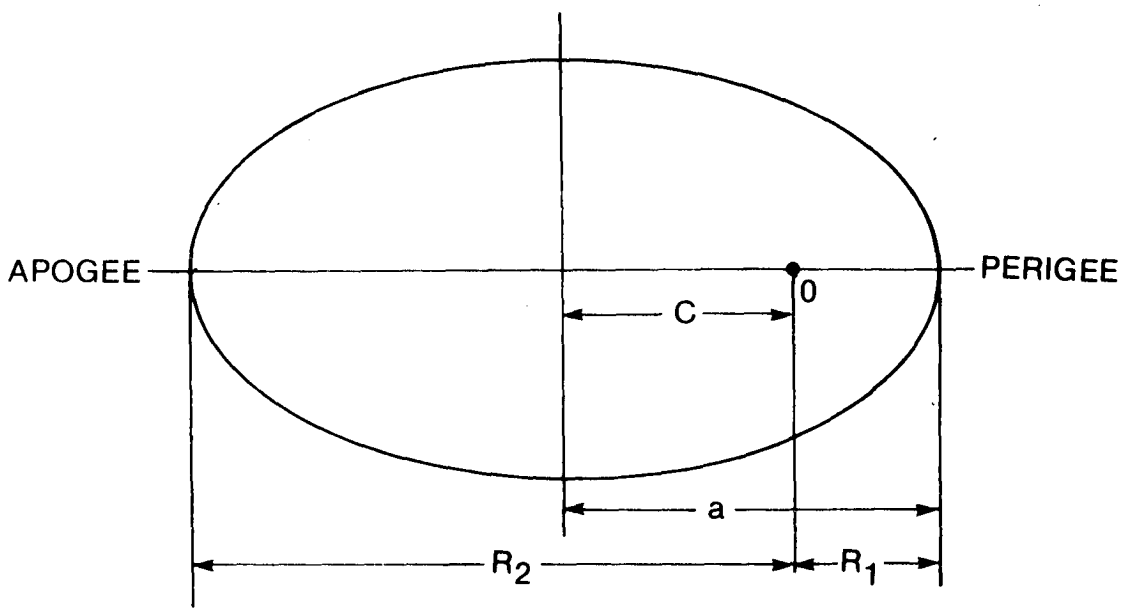

Figure 1. Diagram defining the quantities to describe an elliptical orbit.

At the perigee point the distance R_1 may be broken into the lengths:

$$R_1 = r_e + h_p \tag{1}$$

where r_e is the radius of the Earth, normally taken to be 6.375×10^6 m, and h_p is the height of the satellite above the surface of the Earth. Similarly, the length R_2 may be broken into:

$$R_2 = r_e + h_a \tag{2}$$

where h_a is the height of the satellite above the surface of the Earth at apogee.

The length of the semi-major axis of the ellipse may be determined to be:

$$a = \frac{R_1 + R_2}{2} \tag{3}$$

from which the semi-focal length may be calculated:

$$C = a - R_1 = \frac{R_2 - R_1}{2} \tag{4}$$

From the defining quantities, the eccentricity e, which is a measure of the ellipticity of the orbit, may be given as:

$$e = C/a = \frac{R_2 - R_1}{R_1 + R_2} \tag{5}$$

If $R_1 = R_2$ (i.e. a circular orbit), then e reduces to zero.

At some instant of time t, a polar angle f having a radial distance R is mapped out locating the position of the satellite relative to its perigee as illustrated in Figure 1(a). Also illustrated in this diagram is the orbital co-ordinate system (X_1', X_2', X_3') with its point of origin located at the centre-of-gravity. The X_1'-X_2' plane represents the orbital plane; X_1' is directed towards perigee along the semi-major axis and X_2' is directed perpendicularly outwards from the semi-major axis. The X_3' axis is directed perpendicularly upwards from the orbital plane (i.e. from the plane of the paper) in conformance with a right-handed orthogonal system. The polar angle f, called the true anomaly, is given[1] by:

$$f = \tan^{-1}\left[\frac{\sqrt{1-e^2}\,\sin E}{\cos E - e}\right] \tag{6}$$

The angle E is called the eccentric anomaly and is the solution of the trans-

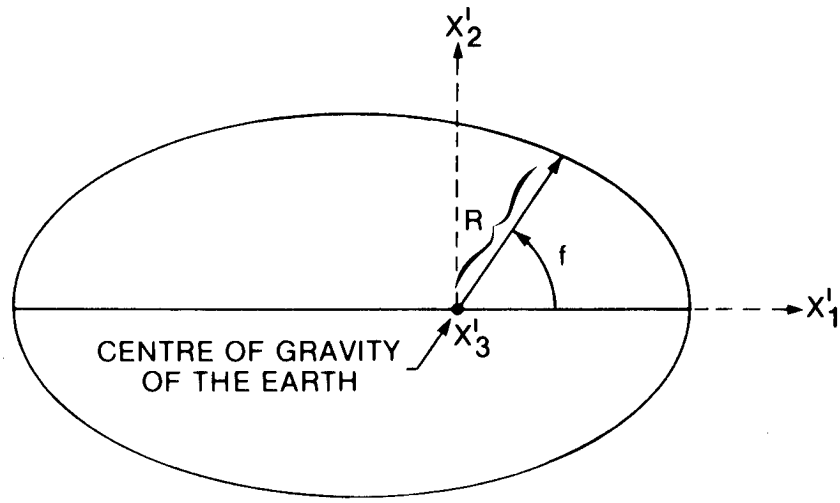

Figure 1(a). Diagram describing the position of a satellite in polar form on an elliptical orbit.

cendental Kepler's equation[1]:

$$E - e \sin E = \left(\frac{\mu}{a^3}\right)^{\frac{1}{2}}(t-T) \tag{7}$$

where μ is the gravitational constant of the Earth (= 3.986008×10^{14} m^3/s^2).

The quantity T in Eqn. (7) is an integration constant that is determined by specifying the time origin. If time is measured from the instant that the satellite is at perigee, then T=0. An expression for the radial distance R may be given in terms of the semi-major axis a, the eccentricity e and the true anomaly f:

$$R = a(1-e^2)/(1 + e \cos f) \tag{8}$$

A1.2 Solving Kepler's Equation

The solution to Kepler's equation (Eqn. (7)), may be found by an iterative process using the Newton-Raphson method to the first order. The equation to be solved for E can be written as:

$$E - e \sin E = M \tag{9}$$

If an initial approximation for E is known, namely E_o, then the next estimate is given by:

$$E_1 = E_o + \Delta E \tag{10}$$

where

$$\Delta E = \frac{M - E_o + e \sin E_o}{1 - e \cos E_o} \tag{11}$$

The next approximation is found by substituting E_1 in place of E_0 and computing a new value for ΔE. This iterative process is then repeated until the desired accuracy in E is obtained.

A1.3 Deduction of Circular Orbits from Elliptical Orbits

In the foregoing mathematical treatment, the general elliptical orbit was considered. Circular orbits are obtained by letting $R_1 = R_2 = R$. Then, as noted earlier, the eccentricity e reduces to zero and from eqns. (3), (6) and (7):

$$f = E = \left(\frac{\mu}{R^3}\right)^{\frac{1}{2}}(t-T) \tag{12}$$

A2 GEOMETRY OF ORBITING SATELLITES

A2.1 Reference Co-ordinate System

Co-ordinate systems which are employed to describe the geometrical positions of satellites can be classified by specifying three items, (1) the origin of the co-ordinates, (2) the reference plane, and (3) the reference direction. In this report we shall use for (1) the centre of the Earth, for (2) the equatorial plane, and for (3) the Greenwich Meridian. With respect to the reference direction, all longitudinal angles are considered to be positive to the east of the Greenwich Meridian and negative to the west. With respect to the reference plane, all latitudinal angles are considered to be positive to the north of the equator and negative to the south.

In Figure 2 is shown a geocentric orthogonal co-ordinate system (X_1,X_2, X_3), where the point of origin is located at the centre of the Earth. The X_1 axis is directed towards the Greenwich Meridian at the equator. The X_1-X_2 plane is the reference equatorial plane. The X_3 axis is directed towards the geometric north pole. The definitions of the remaining symbols are as follows:

θ is the longitudinal angle of the orbital plane at the intersection with the reference plane;

ϕ is the angle in the orbital plane describing the position of P with respect to the line of intersection of the orbital plane with the reference plane;

P is the perigee point, and the position of the satellite at time T=0;

i is the orbital inclination angle relative to the reference plane;

B is some arbitrary point on the orbit indicating the position of the satellite at some instant of time t;

f is the true anomaly measured from the reference position P;

θ_s is the longitudinal angle of B;

ϕ_s is the latitudinal angle of B.

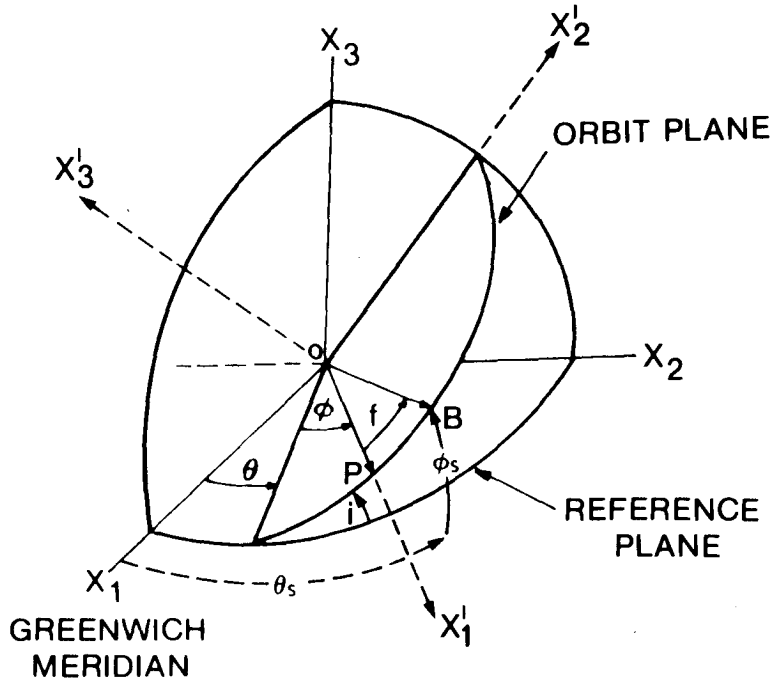

Figure 2. Diagram to illustrate the relationship between an orbital co-ordinate system and a geocentric co-ordinate system.

Let the position of the satellite with respect to the orbital co-ordinate system at the instant of time t be given in component form as:

$$\begin{aligned} X_1' &= R \cos f \\ X_2' &= R \sin f \\ X_3' &= 0 \end{aligned} \tag{13}$$

In order to relate the position of the satellite to the reference geocentric co-ordinate system, three rotations are applied to these components giving:

$$\begin{pmatrix} X_1 \\ X_2 \\ X_3 \end{pmatrix} = R_3(-\theta) \cdot R_1(-i) \cdot R_3(-\phi) \begin{pmatrix} X_1' \\ X_2' \\ X_3' \end{pmatrix} \tag{14}$$

where $R_j(\beta)$, represents an orthogonal matrix describing a counter-clockwise rotation about the jth axis by the angle β as viewed from the positive end of the j^{th} axis, and is defined for the three-axes co-ordinate system as follows:

$$R_{j=1}(\beta) = \begin{pmatrix} 1 & 0 & 0 \\ 0 & \cos\beta & \sin\beta \\ 0 & -\sin\beta & \cos\beta \end{pmatrix} \tag{14A}$$

$$R_{j=2}(\beta) = \begin{pmatrix} \cos\beta & 0 & -\sin\beta \\ 0 & 1 & 0 \\ \sin\beta & 0 & \cos\beta \end{pmatrix} \tag{14B}$$

$$R_{j=3}(\beta) = \begin{pmatrix} \cos\beta & \sin\beta & 0 \\ -\sin\beta & \cos\beta & 0 \\ 0 & 0 & 1 \end{pmatrix} \tag{14C}$$

A2.2 Rotation of the Earth

The Earth rotates in a counter clockwise fashion about the X_3 axis. Since the reference co-ordinates (X_1, X_2, X_3) are fixed with respect to the Earth, this rotation may be represented by a clockwise rate of change in the longitudinal angle θ of the orbital plane,

$$\theta = \theta_o - \omega_t \tag{15}$$

where θ_o is the initial longitude, at t=0, and ω is the angular velocity of the Earth, normally taken to be 7.292×10^{-5} radians/sec. Thus, Eqn. (14) may be rewritten giving:

$$\begin{pmatrix} X_1 \\ X_2 \\ X_3 \end{pmatrix} = R_3(-\theta_o) \cdot R_3(\omega t) \cdot R_1(-i) \cdot R_3(-\phi) \begin{pmatrix} X_1' \\ X_2' \\ X_3' \end{pmatrix} \tag{16}$$

In the pictorial illustrations that follow, this operation has the effect of displacing or twisting the orbit of the satellite as a way of representing the Earth's rotation, while the Earth remains stationary with respect to the observer.

The longitude and latitude of the satellite are given by:

$$\theta_s = \tan^{-1}\left[\frac{X_2}{X_1}\right] \tag{16A}$$

and

$$\phi_s = \sin^{-1}\left[\frac{X_3}{R}\right] \tag{16B}$$

A3 COMPUTATIONAL AND DISPLAY PROCEDURES

A3.1 The Viewpoint

The viewpoint is a chosen location on the Earth's surface at which an observer may view the Earth. The location of the observer is considered to be on a line drawn from the Earth's centre through the viewpoint at a distance such that half the sphere of the Earth is always visible. The viewpoint may be represented by the product of two orthogonal matrices as

$$R_2(\phi_v) \cdot R_3(\theta_v)$$

where ϕ_v and θ_v are the chosen viewpoint's latitudinal and longitudinal angles respectively. These two matrices may be applied to Eqn. (16) as follows:

$$\begin{pmatrix} X_{1v} \\ X_{2v} \\ X_{3v} \end{pmatrix} = R_2(\phi_v) \cdot R_3(\theta_v) \cdot R_3(-\theta_o) \cdot R_3(\omega t) \cdot R_1(-i) \cdot R_3(-\phi) \begin{pmatrix} X_1' \\ X_2' \\ X_3' \end{pmatrix} \tag{17}$$

The position of the satellite is now specified, for display purposes, by a new reference co-ordinate system (X_{1v}, X_{2v}, X_{3v}) where the positive X_{1v} axis is the viewpoint line. Eqn. (17) may be simplified if $\theta_v = \theta_o$, in which case:

$$R_3(\theta_v) \cdot R_3(-\theta_o) = I \tag{18}$$

and

$$\begin{pmatrix} X_{1v} \\ X_{2v} \\ X_{3v} \end{pmatrix} = R_2(\phi_v) \cdot R_3(\omega t) \cdot R_1(-i) \cdot R_3(-\phi) \begin{pmatrix} X_1' \\ X_2' \\ X_3' \end{pmatrix} \tag{19}$$

The effect of this equation is to tilt the reference or equatorial plane by the angle ϕ_v. Thus, an observer may view the surface of the Earth at any aspect angle that is desirable by choosing appropriate values for ϕ_v and $\theta_v(=\theta_o)$.

A3.2 Computation and Display

From the foregoing mathematical development leading to Eqn. (19), a program was written in Fortran IV, using the Tektronix Plot 10 Graphics Library, to simulate and display satellites orbiting the Earth. This simulation has been implemented on the CP-6 central computer at CRC.

Assuming that $\theta_v(=\theta_o)$, ϕ_v, i, ϕ, h_a and h_p have been specified, and that the true anomaly f together with the radial distance R have been calculated, Eqn. (19) is computed. The satellite positions plotted on a computer display terminal are of the components X_{2v} and X_{3v} (i.e., the projections on the X_{2v}-X_{3v} plane). The component X_{1v} is used, together with the magnitude of the X_{2v}, X_{3v} projected vector in relation to the Earth's radius, as a means to determine if the satellite is visible to the observer.

A3.3 Computation and Display of Latitudinal and Longitudinal Grid Lines

In order to compute the longitudinal and latitudinal grid lines on the surface of the Earth in relation to the viewpoint, a column matrix is first set up in component form as:

$$\begin{aligned} X_1 &= r_e \cos\alpha \cdot \cos\beta \\ X_2 &= r_e \sin\alpha \cdot \cos\beta \\ X_3 &= r_e \sin\beta \end{aligned} \tag{20}$$

where for any point on the grid α is the longitudinal angle relative to the Greenwich Meridian and β is the latitudinal angle relative to the equatorial plane. Then after matrix rotation into the viewpoint reference system the resulting components are:

$$\begin{pmatrix} X_{1v} \\ X_{2v} \\ X_{3v} \end{pmatrix} = R_2(\phi_v) \cdot R_3(\theta_v) \begin{pmatrix} X_1 \\ X_2 \\ X_3 \end{pmatrix} \tag{21}$$

The grid lines can then be plotted in the same manner as previously described for the satellite positions.

A3.4 Resulting Displays of Various Satellite Orbits

In Figure 3 is given an example of the display of a circular polar orbit (i.e., inclination angle i = 90°), where the height of the satellite was 1669 km. The longitudinal and latitudinal grid lines drawn on the surface of the Earth are at increments of 15°, the solid line indicating the reference or equatorial plane. The viewpoint, indicated by the cross which is visible behind the orbital path, is on the 45° latitude grid line. The height of this satellite was chosen so that there are exactly 12 orbits per revolution of the Earth. Thus, for one complete orbit, the Earth rotates 1/12 of one revolution or 30°. This is shown in the figure by the displacement in the angular position of the satellite (a recession of 30°) at the end of the first orbit relative to its starting position at the equatorial plane. In fact, the Earth advances by 30° relative to the orbital plane in the time that has been taken for the satellite to complete one orbit. In Figure 4, a similar result is shown except that the inclination angle i is 45°. The cross, which locates the viewpoint, is now clearly visible.

In Figure 5 is given a plot of an elliptical polar orbit. The height of the satellite at perigee, the south pole, is 250 km and at apogee, the north pole, is 1669 km. Again, the viewpoint, indicated by the cross, is on the 45° latitude grid line. In Figure 6, a similar result is shown except that the inclination angle i is 45°.

In Figure 7, an example is given of a constellation of 8 satellites of heights of 4000 km in different circular polar orbital planes for a non-rotating Earth. The stars represent the positions of the satellites at some instant of time t.

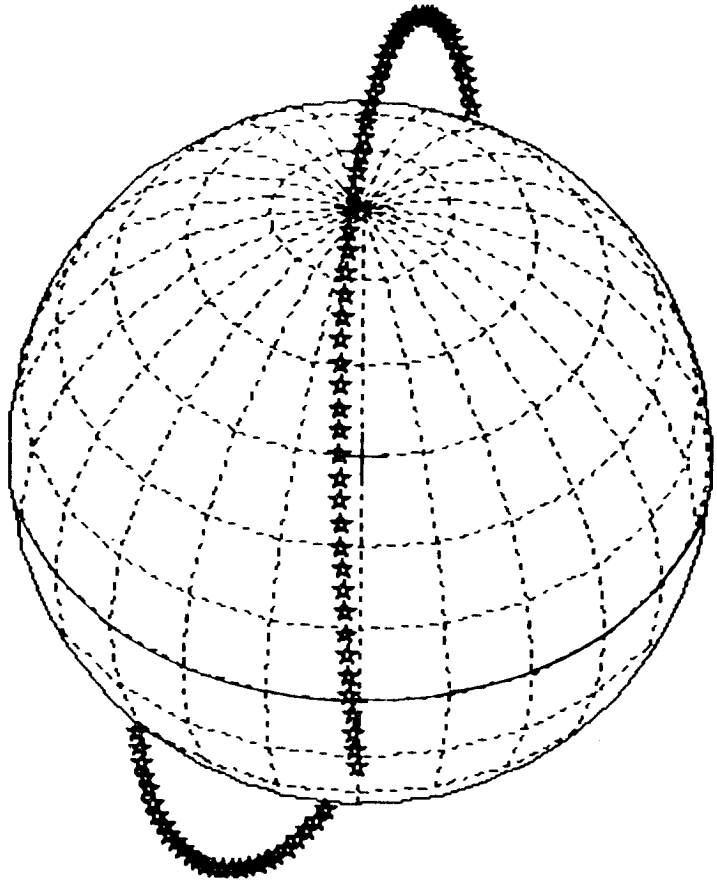

Figure 3. Polar circular orbit of a satellite of height of 1669 km; $\phi_V = 45^\circ$.

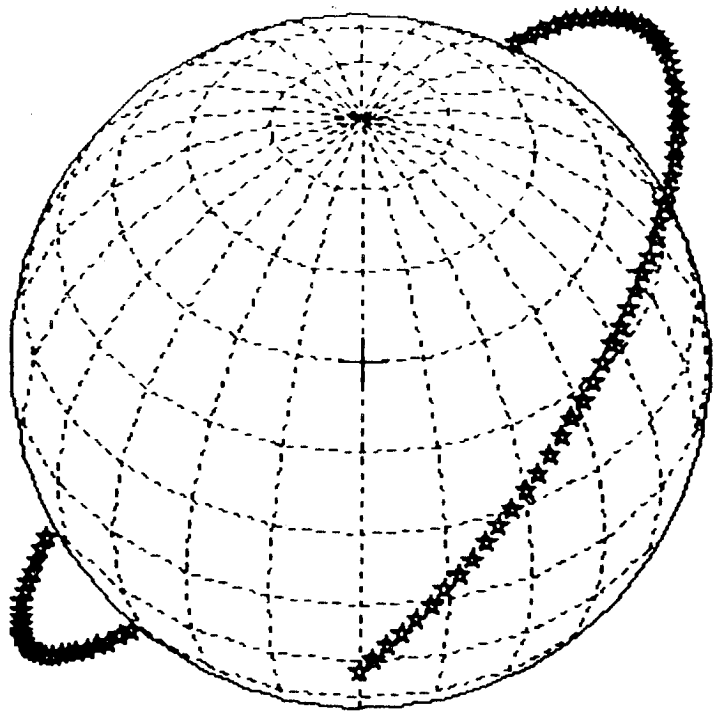

Figure 4. Circular orbit of a satellite of height of 1669 km inclined by 45° relative to the equatorial plane; $\phi_V = 45^\circ$.

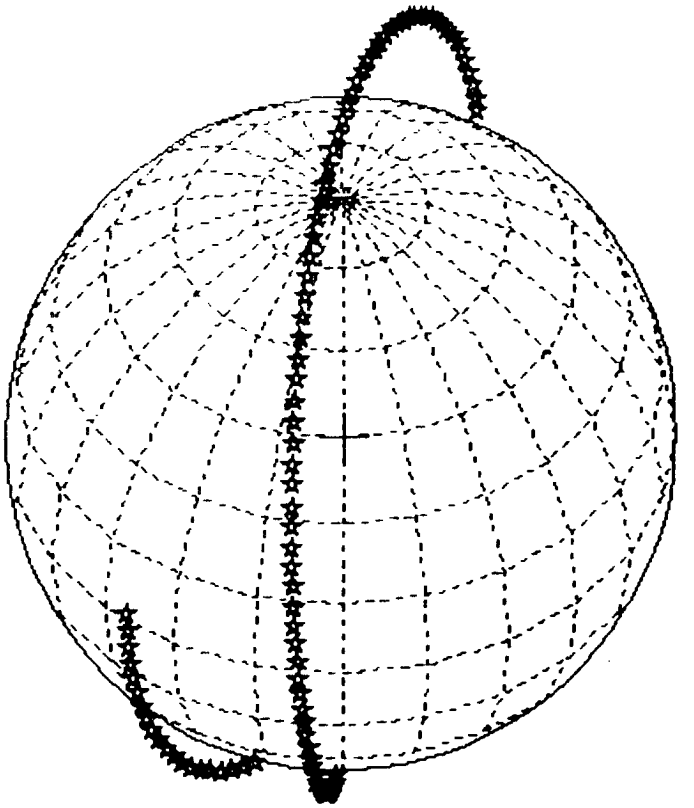

Figure 5. Elliptical polar orbit. Satellite height at perigee (south pole) is 250 km. Satellite height at apogee (north pole) is 1669 km; $\phi_V = 45^\circ$.

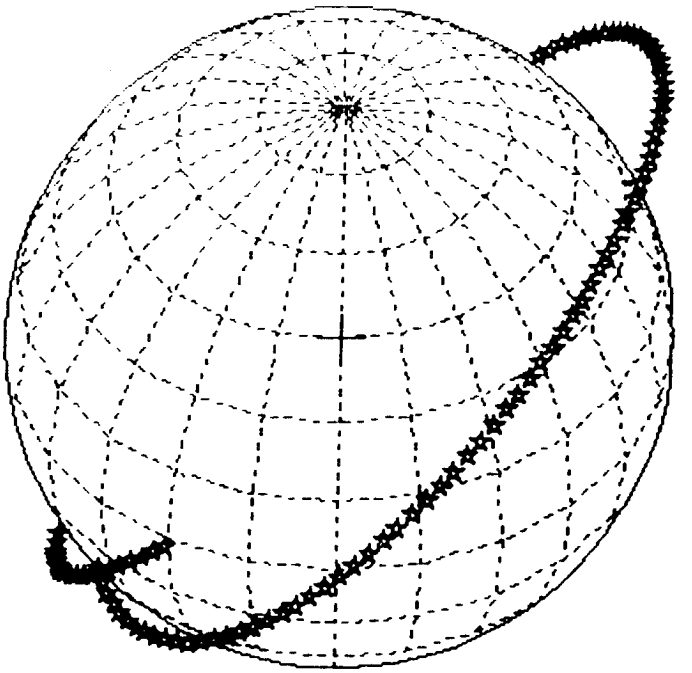

Figure 6. Elliptical orbit inclined at 45° to the equatorial plane. Satellite height at perigee is 250 km. Satellite height at apogee is 1669 km; $\phi_V = 45^\circ$.

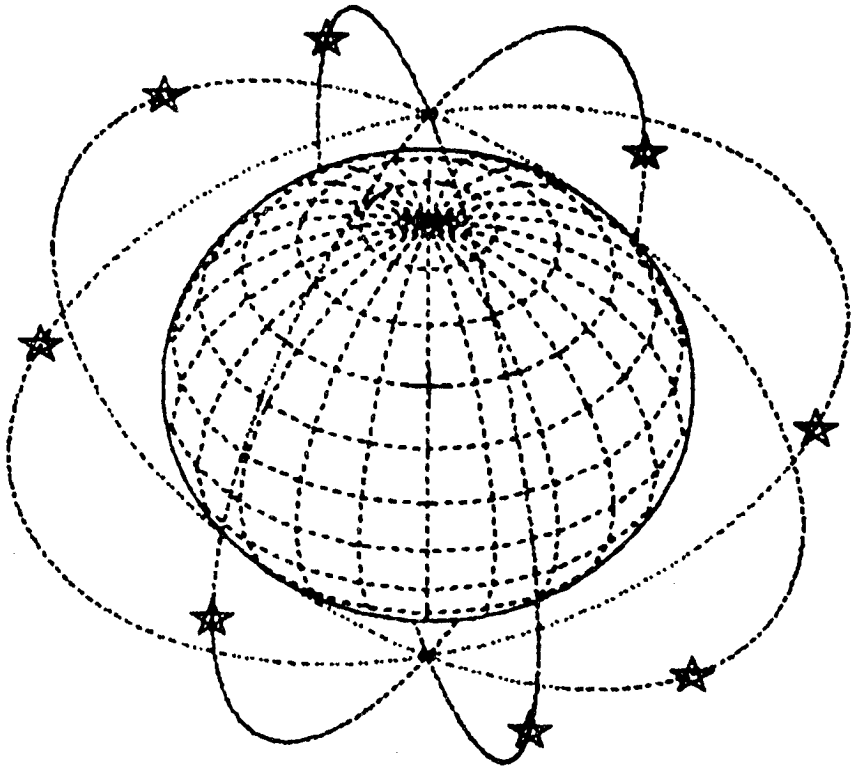

Figure 7. Polar circular orbit of 8 satellites of heights of 4000 km in different orbital planes; $\phi_v = 45°$.

PART B - LONG-TERM EARTH COVERAGE STATISTICS

B1 FIELDS OF VIEW AND COVERAGE AREAS

In dealing with fields of view and Earth coverage areas, consider that there is a radar system aboard the satellite which is orbiting the Earth. The field of view is defined as the instantaneous area of the surface of the Earth in which the radar can theoretically detect the radial velocity component of a moving target by Doppler processing.

B1.1 Computation of the Field of View

At some instant of time t the satellite is located at the point B on the X_1'-X_2' orbital plane as shown in Figure 8. The angle f is computed from the transcendental equation of time from the perigee point at the X_1' axis; r_e is the Earth's radius and h is the height of the satellite. The angle A is the antenna pointing angle described for a point S at the Earth's surface corresponding to the grazing angle γ and is then obtained from the law of sines:

$$A = \sin^{-1}\left[\frac{\cos\gamma}{1+h/r_e}\right] , \qquad (22)$$

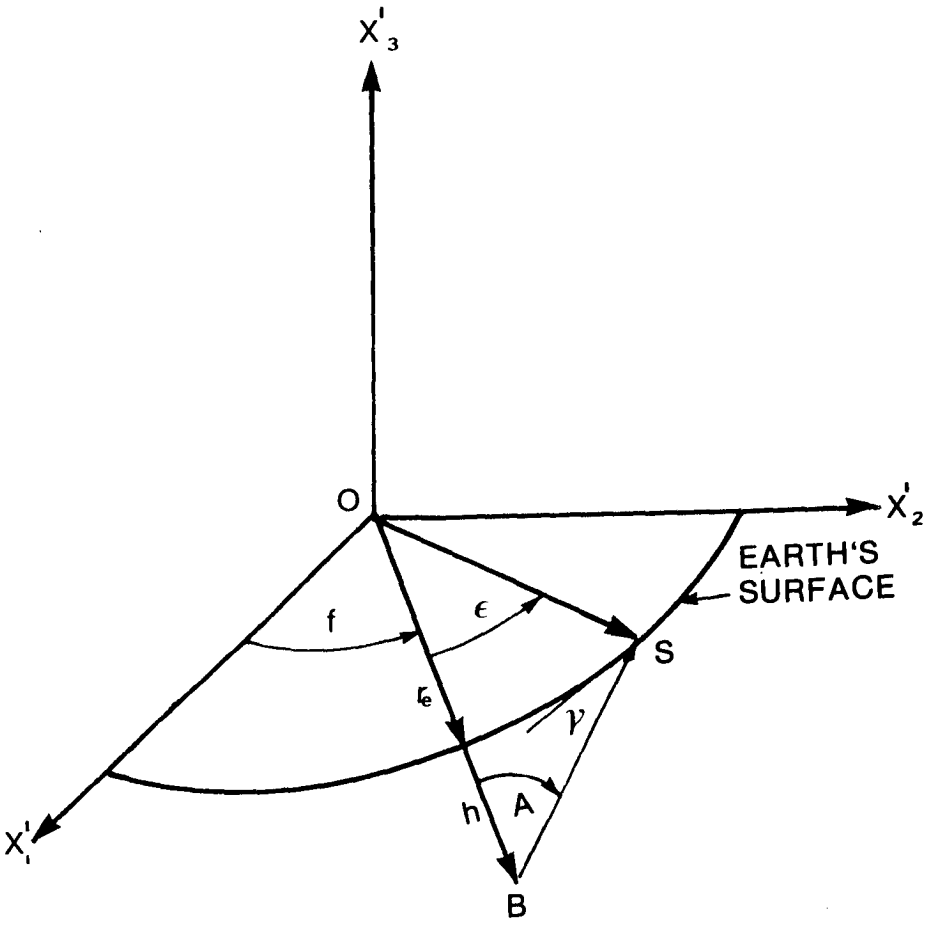

Figure 8. Illustration of the co-ordinate system used for computing the field of view.

from which the angle ε, subtended at 0 by the line BS, may be determined:

$$\varepsilon = 90 - \gamma - A \text{ degrees.} \tag{23}$$

With this geometrical configuration, the field of view on the surface of the Earth covered by all grazing angles greater than γ (or equivalently, by pointing angles less than A) can be mapped out by a 360° rotation of the vector BS about the axis OB. By methods analogous to the procedure described in Section A3.3 the result of this operation can be displayed with respect to the viewpoint reference co-ordinate system.

The field of view may be specified by means of a minimum and a maximum grazing angle. The minimum grazing angle, γ_{min}, is chosen based on antenna beamwidth considerations and in this study is taken to be 5°. The maximum grazing angle, γ_{max}, is chosen such that for values of $\gamma > \gamma_{max}$ the radial velocity component of a moving target would be too small to be detected by the radar. Thus, the theoretical field of view is bounded by an outer and an inner circle, where the surface inside the inner circle, known as the Nadir hole, is an area where radar coverage of moving targets is theoretically not possible. In this study, γ_{max} is taken to be 60°.

B1.2 Resulting Displays for Different Satellite Orbits

In Figure 9, a picture is given of the field of view on the surface of the Earth shown by the area inside the solid lines. The satellite, indicated by the star, was located over the north pole at a height of 2000 km. In Figure 10, a similar picture is shown for a satellite height of 4000 km. These examples show how the field of view increases with the height of the satellite.

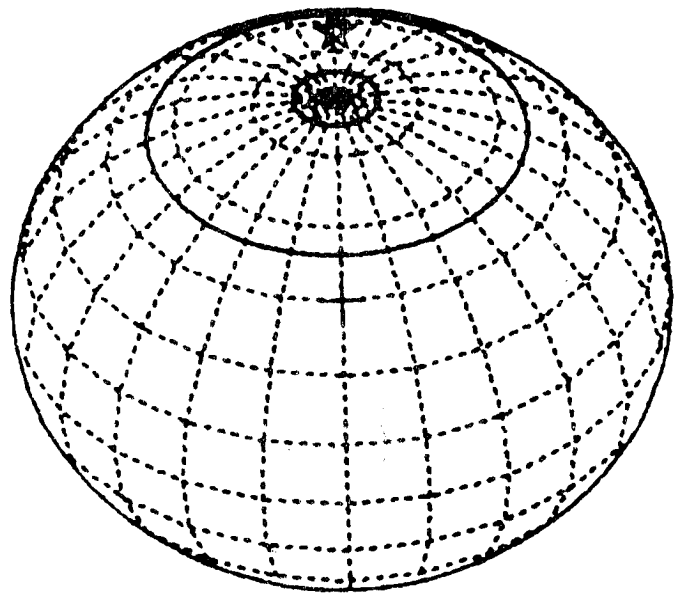

Figure 9. Plot of the field of view for a satellite height of 2000 km; located over the north pole; $\gamma_{min} = 5^{\circ}$; $\gamma_{max} = 60^{\circ}$; $\phi_V = 45^{\circ}$.

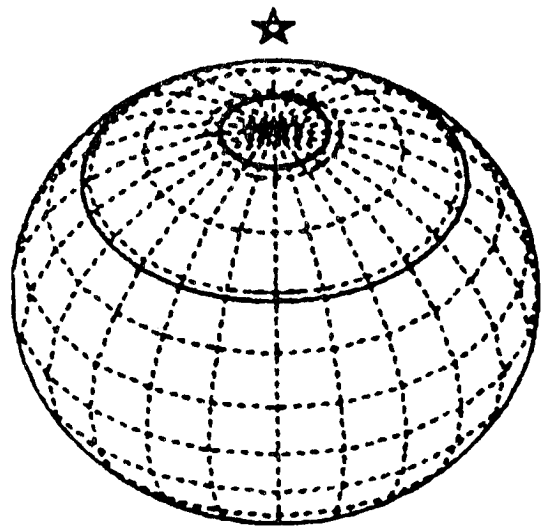

Figure 10. Plot of the field of view for a satellite height of 4000 km located over the north pole; $\gamma_{min} = 5^{\circ}$; $\gamma_{max} = 60^{\circ}$; $\phi_V = 45^{\circ}$.

This relationship is shown quantitatively in Figure 11 where the percent coverage area in the field of view to that of the total surface area of the Earth is plotted against increasing satellite height. The curve, labelled 1, includes that of the surface area of the Nadir hole whereas Curve 2 excludes it. The divergence of the two curves indicates the increase in the surface area of the Nadir hole with increasing satellite height. In Figure 12, a plot is given of the lowest latitude to which coverage is provided against increasing satellite height for a satellite located over the North Pole. For example, at a height of 2000 km, the lowest latitude is 54° whereas at a height of 10000 km, the lowest latitude is 28°.

B2 CONSTELLATION OF SATELLITES FOR CONTINUOUS COVERAGE

In order to provide for continuous coverage of a point on the Earth using non-geostationary orbits, a constellation of satellites is required. The number of satellites required in the constellation is determined by first realizing that their fields of view must overlap one another by at least 50% in order to take into account the effect of the Nadir hole.

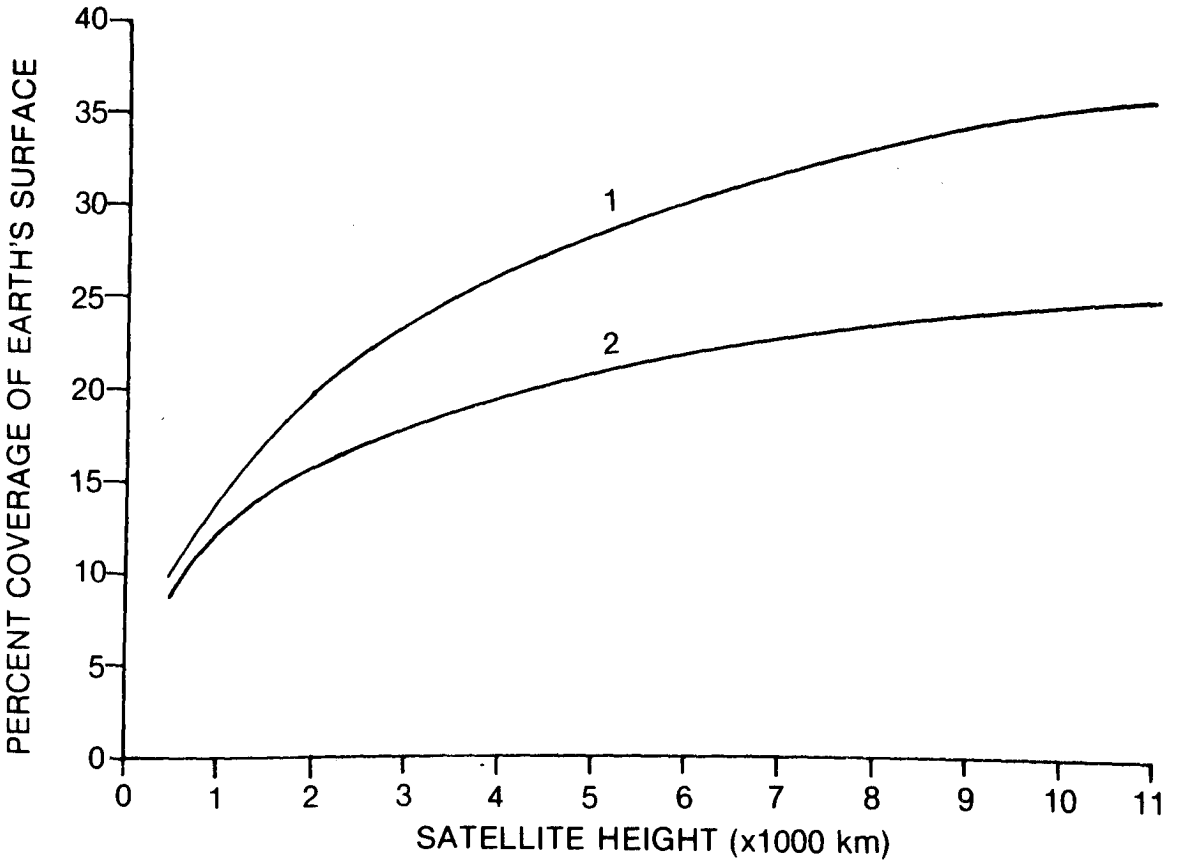

Figure 11. Plot of percent coverage area against satellite height.

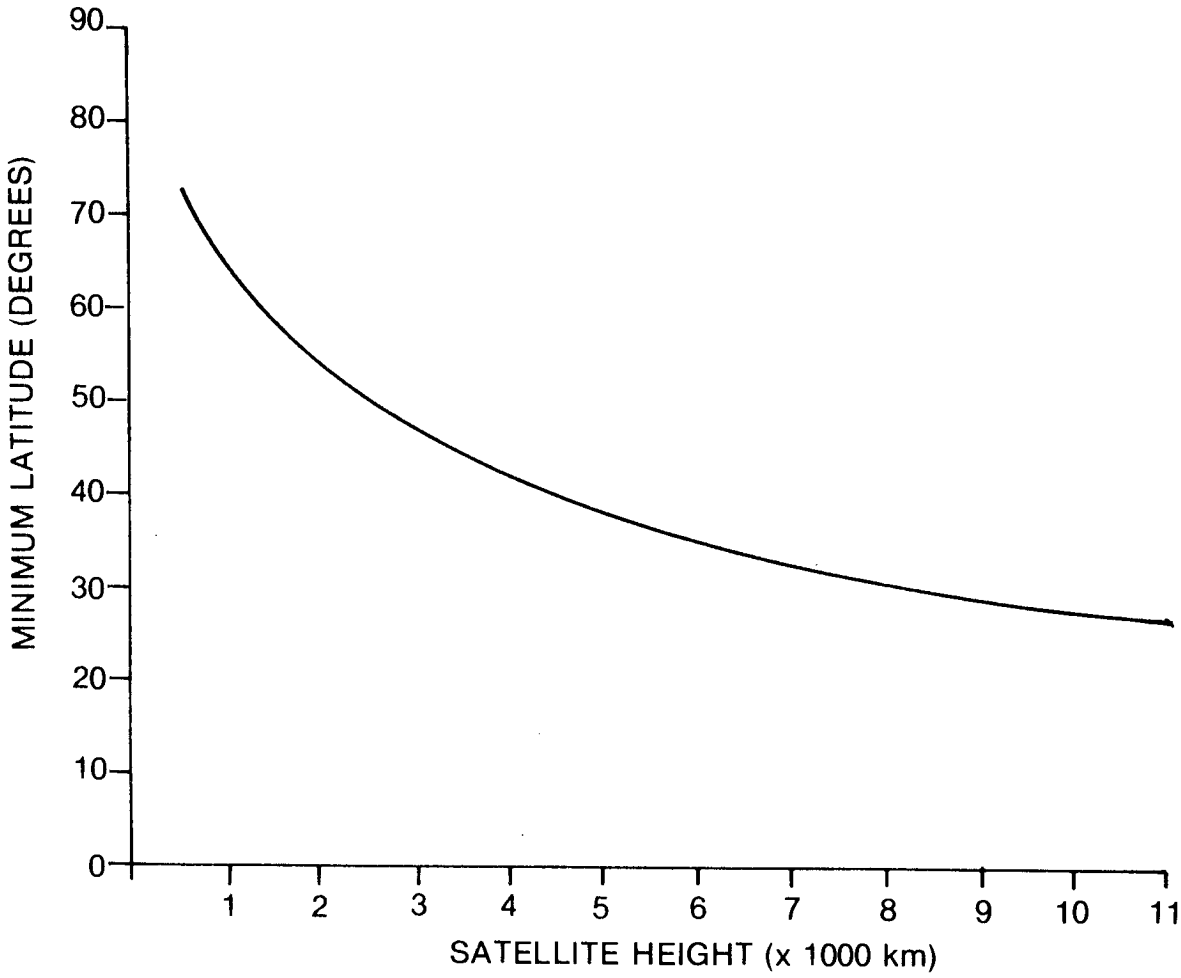

Figure 12. Plot of minimum latitude against satellite height.

B2.1 Diagrams of Continuous Coverage

In Figure 13 the overlapping fields of view are illustrated for a constellation of eight satellites in circular polar orbit of height 5000 km on a single orbital plane. The viewpoint is at the equatorial plane but viewed along the line of the orbital plane. Only five out of the eight satellites are in view. In Figure 14, the same configuration is shown when viewed perpendicularly to the orbital plane. It should be noted that the zone on the Earth's surface bounded by the octagonal edges is an area where no coverage is possible. This no-coverage zone moves as the Earth rotates with respect to the orbital plane of the satellites and sweeps out a band around the Earth where coverage is intermittent. For a polar-orbiting constellation in a single plane, this is an equatorial band bounded by the appropriate "lowest-latitude" values (north and south) obtained from Figure 12.

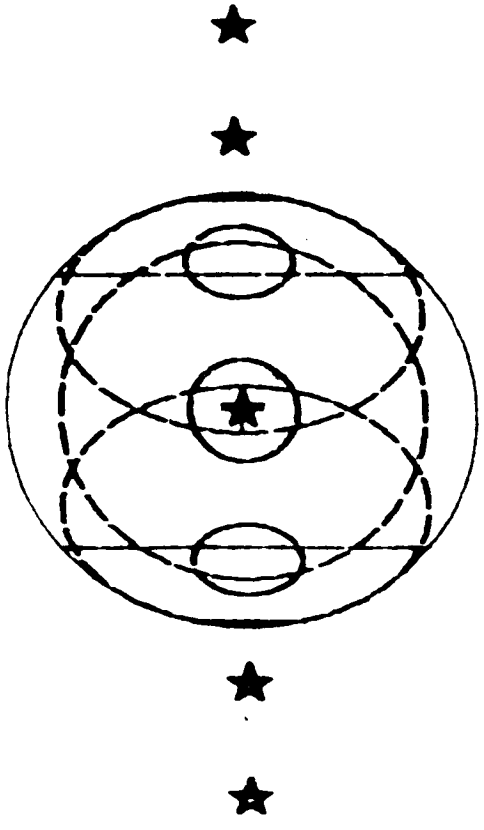

Figure 13. Diagram of continuous coverage viewed along the line of the orbit consisting of 8 satellites of heights of 5000 km and spaced equi-distant from one another; $\phi_V = 0.0^\circ$.

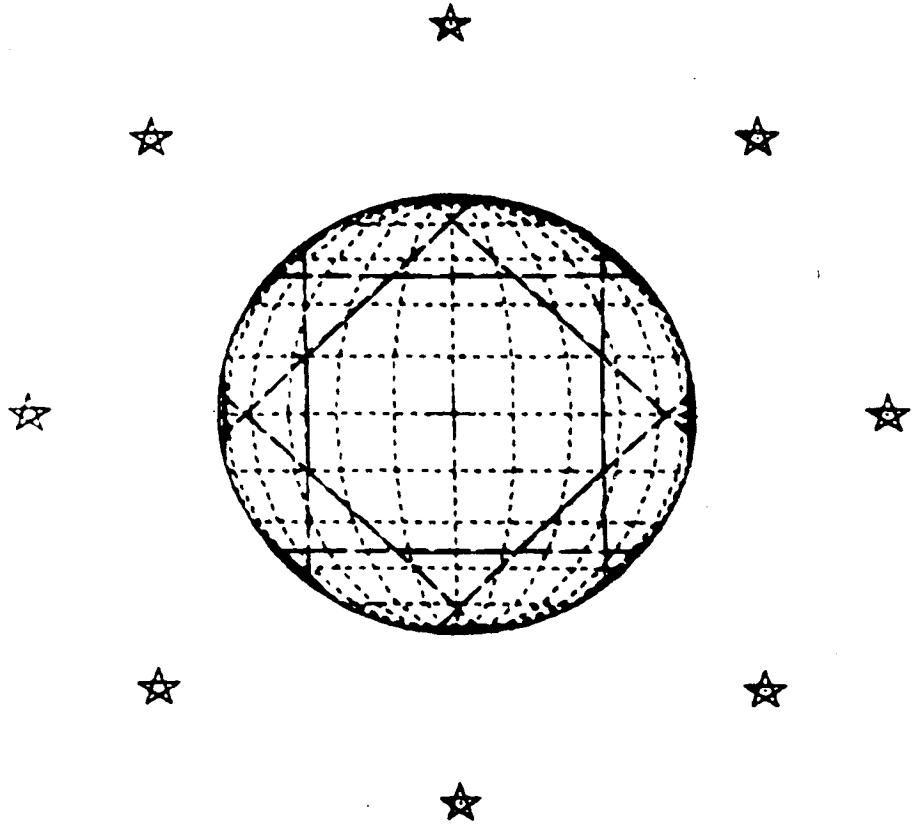

Figure 14. Diagram of continuous coverage viewed perpendicularly to the orbital plane consisting of 8 satellites of heights of 5000 km and spaced equi-distant from one another; $\phi_V = 0.0^\circ$.

In Figure 15 the overlapping fields of view are shown for a similar constellation of six satellites of height 10000 km. Again, the viewpoint is at the equatorial plane but viewed along the line of the orbital plane. Only four of the six satellites are in view. In Figure 16, the same configuration is shown when viewed perpendicularly to the orbital plane. The curve in Figure 12 shows how the zone of intermittent coverage decreases with increasing satellite height.

In Figure 17, a plot is given of the number of satellites in circular polar orbit required to provide continuous coverage against the height of the satellite. For example, for a satellite height of 2000 km, eleven satellites would be required to provide continuous coverage whereas for a satellite height of 10000 km only six would be required. From Figure 12, this continuous coverage would extend down to 54° latitude in the former case and 28° latitude in the latter.

B3 LONG-TERM COVERAGE STATISTICS FOR DIFFERENT ORBITAL CONFIGURATIONS

Examples are given of the sort of long-term coverage statistics that can be obtained using this computer-based analytical tool, as a means of comparing different orbital configurations. These statistics were compiled over a simulated 24 hour period, giving coverage as a function of target latitude. The "target" was considered to be a stationary point on the surface of the Earth, rotating with the Earth.

B3.1 Orbital Configurations

The first two experiments consisted of six radar satellites at a height of 10000 km uniformly distributed in a circular polar orbit, aligned (1) in a single orbital plane and (2) in multiple orbital planes. The results of these two experiments are shown in Figure 18.

The second two experiments consisted of six radar satellites distributed at equal intervals in time in an elliptical polar orbit where the height at perigee, the south pole, was 500 km and at apogee was 10000 km. The satellites were aligned (1) in a single orbital plane and (2) in multiple orbital planes. The results of these two experiments are shown in Figure 19.

B3.2 Discussion of Results

In the example of circular orbits, the satellite constellation in a single orbital plane provided long-term continuous coverage down to a latitude of 35°, whereas for multi-orbital planes long-term coverage generally decreased with decreasing latitude. For latitudes less than 27°, the coverage statistics are slightly better for the multi-orbital configuration. For the elliptical orbit case, long-term coverage was provided by the single orbital plane and the multi-orbital planes down to latitudes of 30° and 32° respectively. For latitudes less than 29°, coverage statistics are slightly better for the multi-orbital configuration.

It is also possible, using this computer simulation, to examine directly the time-dependent coverage pattern of any specified configuration of satellites. For instance, the scale and extent of multiple coverage over

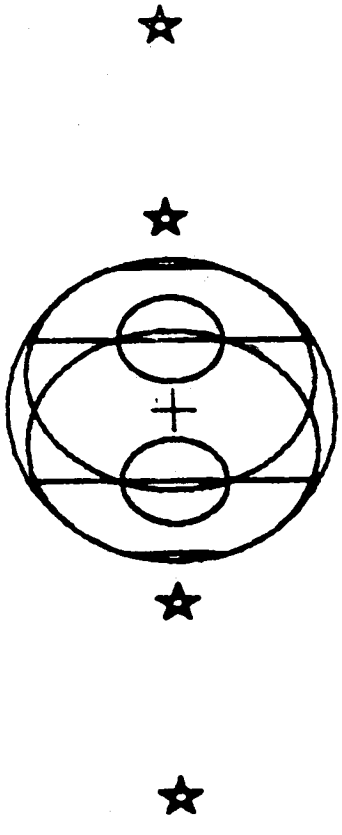

Figure 15. Diagram of continuous coverage viewed along the line of the orbit consisting of 6 satellites at heights of 10000 km and spaced equi-distant from one another; $\phi_v = 0.0^\circ$.

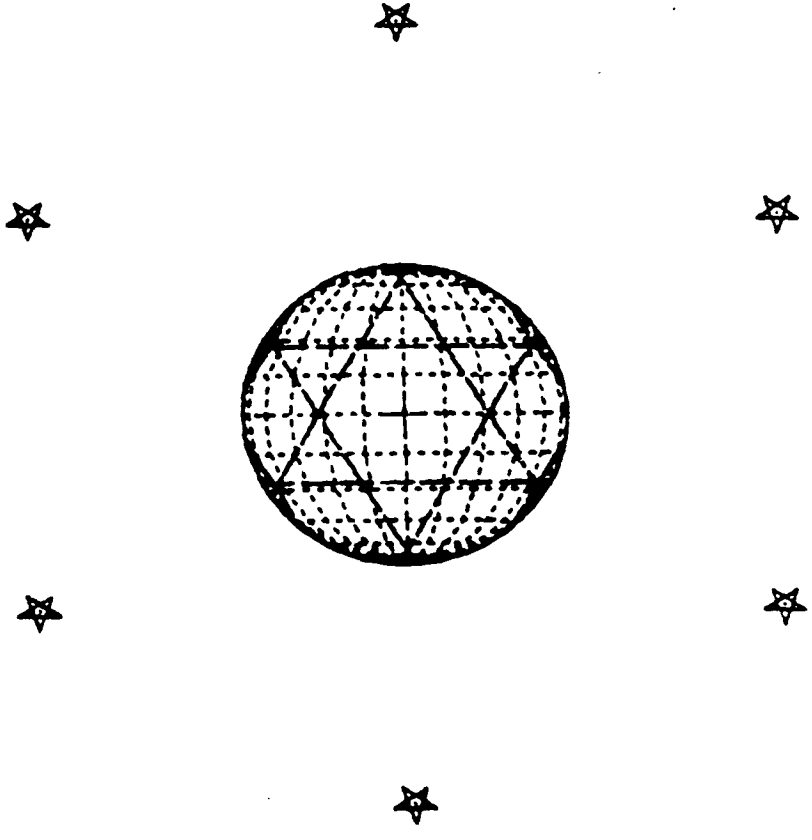

Figure 16. Diagram of continuous coverage viewed perpendicular to the orbital plane consisting of 6 satellites at heights of 10000 km and spaced equi-distant from one another; $\phi_v = 0.0^\circ$.

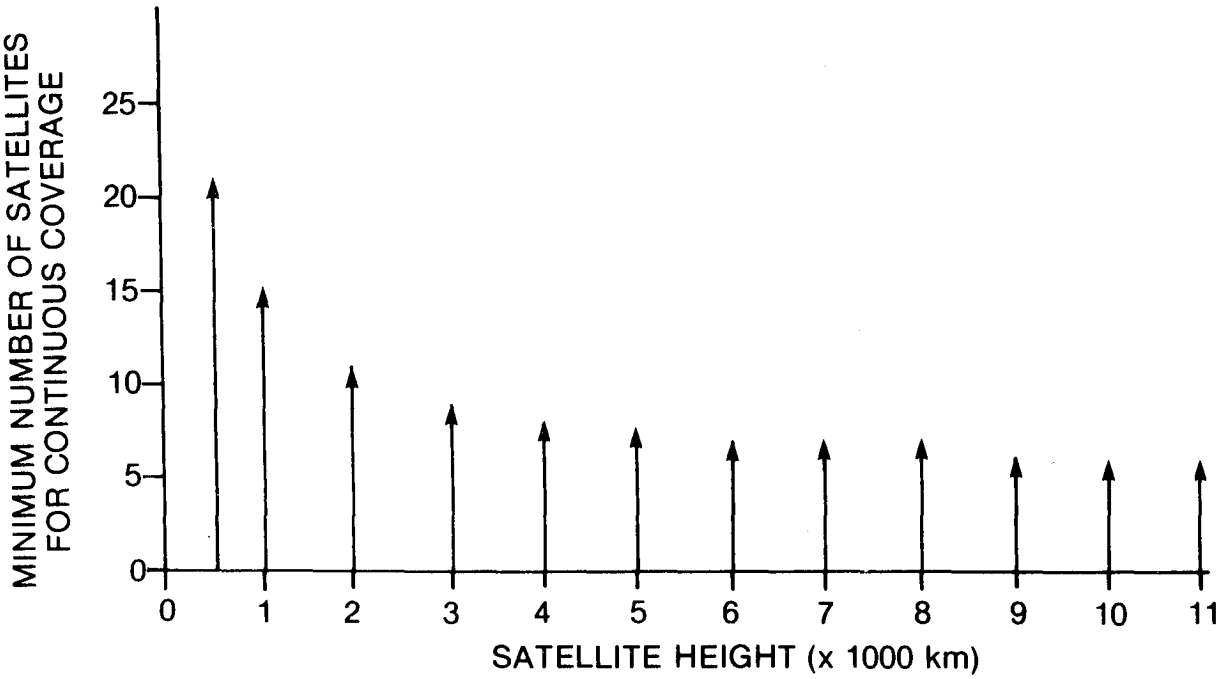

Figure 17. Minimum number of satellites to provide continuous coverage against satellite height.

a certain region of the Earth may be of interest. In this regard, a satellite in elliptical orbit maintains longer coverage times per orbit over a designated area than one in circular orbit, and when multiple satellites are uniformly distributed in time in such orbits, they offer increased occurrence of overlapping coverage of that area.

The choice of a particular configuration of satellites will depend on a number of factors, including mission requirements of the SBR system power-aperture constraints of the radar, spacecraft system considerations, orbital perturbations, etc. This computer-based analysis of the theoretically achievable coverage will contribute to the selection of the most appropriate configuration.

SUMMARY

A description has been given of a computer-based analytical tool intended for the simulation of space-based radar systems for surveillance and tracking of air-breathing targets. This simulation has been used to carry out some preliminary studies of long-term coverage of the Earth's surface for different satellite orbits and configurations, and its usefulness for the evaluation and comparison of proposed SBR systems has been demonstrated with several examples taken from these studies.

Further studies are in progress, in which the detection performance of the SBR system for moving targets against Earth clutter is included in the cover-

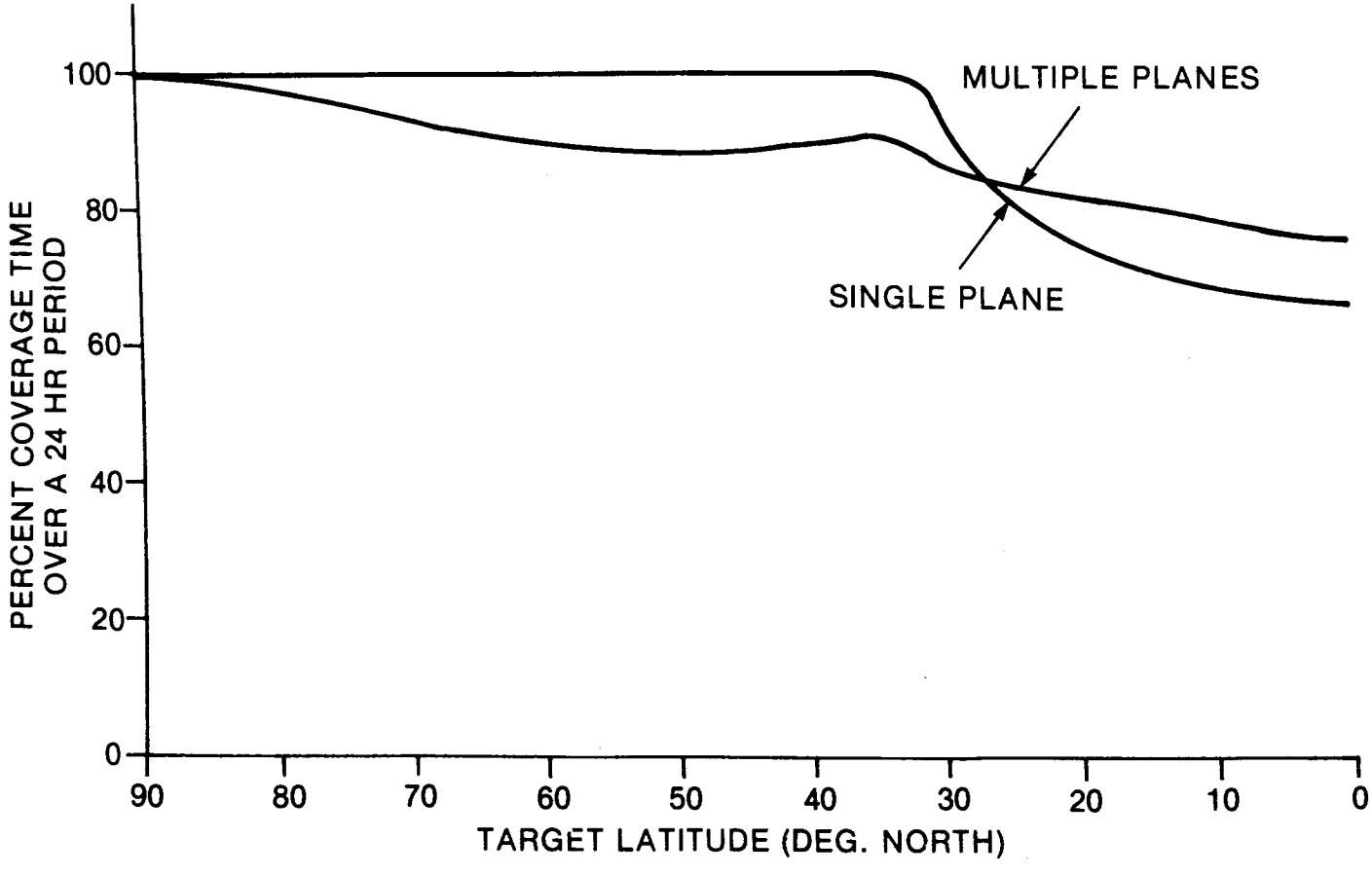

Figure 18. Long-term coverage statistics for circular polar orbits of heights of 10000 km.

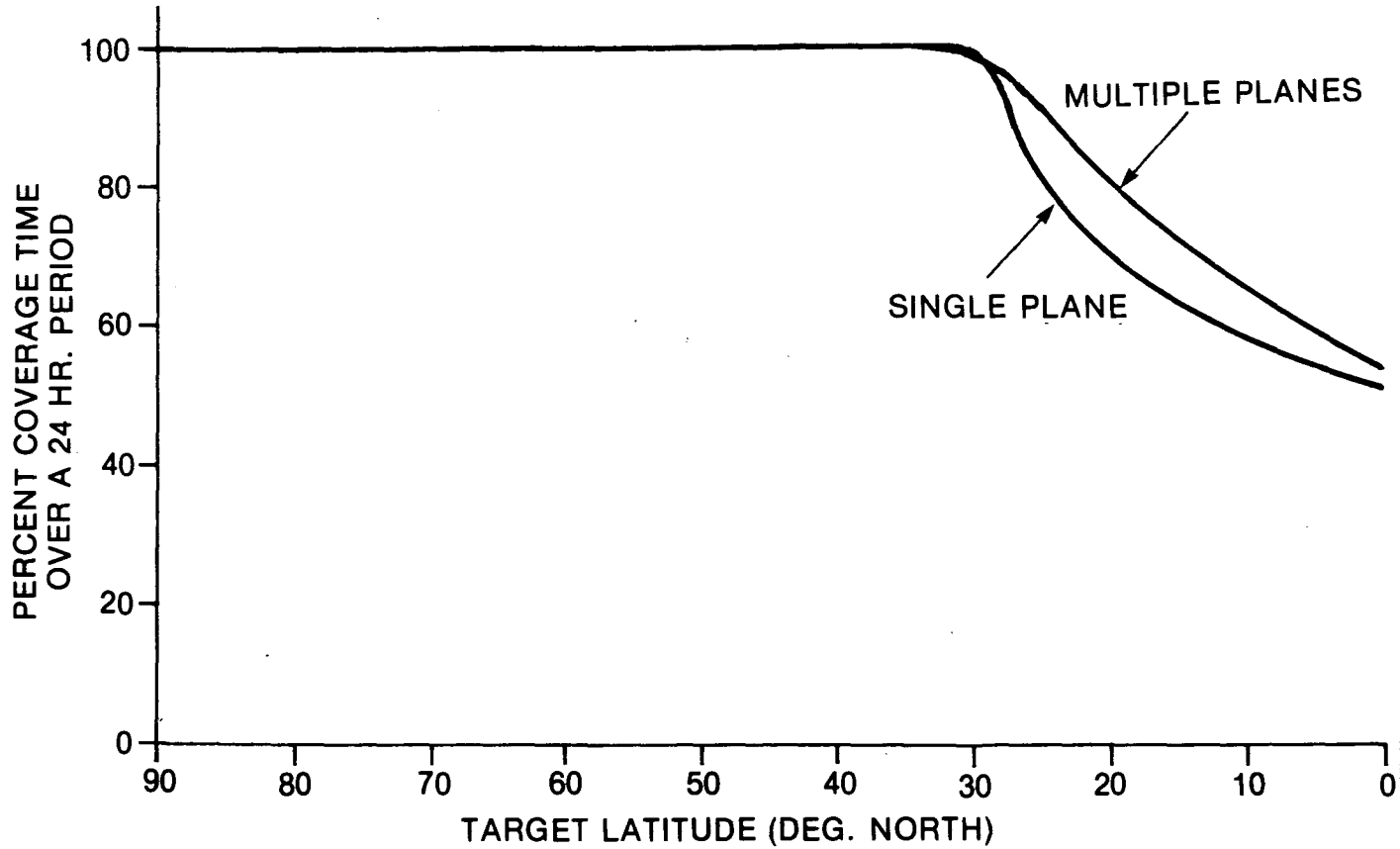

Figure 19. Long-term coverage statistics for elliptical polar orbits h_p (south pole) = 500 km, h_a = 10000 km.

age analysis. For these studies, which will be described in a future report, the computer simulation is augmented to include the radar parameters, target characteristics and a model for Earth clutter as seen from a space-based radar.

ACKNOWLEDGEMENT

The author acknowledges the contribution of Dr. N. Brousseau, Dr. A.W. Bridgewater and Mr. R.H. Martin during the course of this work.

REFERENCES

1. Deutsch, R., *Orbital Dynamics of Space Vehicles*, Prentice-Hall, 1963, Chapters 1-2.